Benzilmonoximethiocarbohydrazide Schiff Bases as Multifunctional Antimalarial and Antioxidant Scaffolds: Synthesis, Biological Evaluation, and Mechanistic Insights

Shravan Kumar Singh‡[1], Abhay Bagul‡[2], Manish Kumar[3], Aisha Tufail[4], Santosh Waman Kulkarni[5], Sheetal Sharma[1,] and Amit Dubey[6,] ✉

[1]Department of Chemistry, Lovely Professional University, Phagwara, -144411, Punjab, India

[2]Department of Chemistry, VasantraoNaikMahavidhyalaya, Aurangabad 431003, Maharashtra, India

[3]Department of Biochemistry, Iswar Saran Degree College, University of Allahabad (A Constituent PG College of University of Allahabad), Prayagraj, India.

[4]Computational Chemistry and Drug Discovery Division, Quanta Calculus, Greater Noida-201310, Uttar Pradesh, India

[5]K. M. Agrawal College of Arts, Commerce & Science, Kalyan (W), Thane, University of Mumbai 421301, Maharashtra, India.

[6]Center for Global Health Research, Saveetha Medical College and Hospitals, Saveetha Institute of Medical and Technical Sciences, Chennai, Tamil Nadu, India.

✉**Corresponding Author:**

Amit Dubey, Center for Global Health Research, Saveetha Medical College and Hospitals,

Saveetha Institute of Medical and Technical Sciences, Chennai, Tamil Nadu, India.

Institutional Email: amitdubey@saveetha.com

Email:ameetbioinfo@gmail.com

‡ Equal Contribution

Table S1: Global Reactivity Descriptors Derived from DFT Calculations of HBMT Analogues

Descriptor	HBMT-MA3	HBMT-MA6	HBMT-MA7	HBMT-3M4HB	Units	Formula / Definition
Total Energy (E_{total})	–1678.8573	–1623.7831	–1662.7832	–1773.2762	Hartree	Optimized energy of entire molecule
Binding Energy	–10.5940	–10.1307	–10.7102	–10.5758	Hartree	Stabilization energy upon formation
HOMO Energy (E_{HOMO})	–0.1692	–0.1466	–0.1572	–0.1628	Hartree	Highest occupied molecular orbital
LUMO Energy (E_{LUMO})	–0.1063	–0.1076	–0.1100	–0.1084	Hartree	Lowest unoccupied molecular orbital
HOMO–LUMO Gap (ΔE_{gap})	0.0629	0.0390	0.0472	0.0544	Hartree	$\Delta E = E_{LUMO} – E_{HOMO}$
Electronegativity (χ)	0.1377	0.1271	0.1336	0.1356	Hartree	$\chi = –(E_{HOMO} + E_{LUMO})/2$
Chemical Potential (μ)	–0.1377	–0.1271	–0.1336	–0.1356	Hartree	$\mu = –\chi$
Global Hardness (η)	0.0314	0.0195	0.0236	0.0272	Hartree	$\eta = (E_{LUMO} – E_{HOMO})/2$
Global Softness (S)	31.85	51.28	42.37	36.76	1/Hartree	$S = 1/\eta$
Electrophilicity Index (ω)	0.3017	0.4140	0.3777	0.3374	Hartree	$\omega = \mu^2 / 2\eta$
Dipole Moment Magnitude	3.1267	2.8445	2.9979	3.3352	Debye	Degree of molecular polarity

Note: Absolute total energies differ due to varying atom counts; relative parameters (ΔEgap, hardness, electrophilicity) are more informative for comparing stability.

Table S2: Molecular Electrostatic Potential (MESP) and Reactivity Descriptor Summary of HBMT Analogues

Compound	Global Min	Global Max	ESP Ra	Avg. ES	Most Negative	Most Positive	Dipole Mo	Electrophilic Sites	Nucleophilic Sites	Predicted Interacti

	. ESP (a.u.)	. ESP (a.u.)	nge (a.u.)	P (a.u.)	Region	Region	ment (Debye)			on Tendency
HBMT-MA3	–0.0412	+0.0526	0.0938	–0.0052	C=O, aromatic O atoms	–NH2, imine proton	3.1267	Carbonyl & amide oxygen	NH, aromatic ring edges	Moderate H-bonding and π–π stacking
HBMT-MA6	–0.0465	+0.0581	0.1046	–0.0084	Carbonyl & phenol oxygen	NH groups	2.8445	Phenolic O, ketones	Imine & NH groups	Strong polar and H-bond interactions
HBMT-MA7	–0.0398	+0.0602	0.1000	–0.0061	Ketone and imine oxygen	Amino protons	2.9979	Aromatic ketones	NH2 and benzene ring	Balanced polar and π interactions
HBMT-3M4HB	–0.0483	+0.0565	0.1048	–0.0073	Conjugated C=O and O–H	Amine hydrogens	3.3352	Multiple C=O, phenolic O	NH, CH regions	Strongest H-bond donor/acceptor balance

Table S3. Comparative Molecular Docking Interactions of HBMT Derivatives and Control Drugs with Malarial Protein (PDB ID: 5JWA)

Compound	Docking Energy (kcal/mol)	Key Interacting Residues	Interaction Types	Binding Pocket Description	Inhibitory Potential
HBMT3M4HB	**–9.0**	THR66, THR64, THR423, ASP342, TRP338, ALA424, ALA427, ALA296, LEU299, SER297	H-bonding, π–anion, π–π T-shaped, π–alkyl, van der Waals	Strong hydrogen bonding network, deep π–anion anchoring, and aromatic stacking; stabilized by surrounding hydrophobics	**Very Strong**
HBMT-MA3	**–9.2**	SER58, SER59, LYS156,	H-bonding, π–anion, π–π stacking,	Rich polar interactions with ASP	**Very Strong**

		ASP342, ASP157, TRP338, ALA424, ALA427, VAL136	π–alkyl, van der Waals, positive–positive (repulsion)	residues and TRP stacking, slightly destabilized by LYS156	
HBMT-MA6	**–8.5**	GLY137, VAL136, ASP342, ARG60, PRO459, LYS156, THR302, GLY35	H-bonding, π–cation, π–alkyl, van der Waals, positive–positive (repulsion)	Electrostatic anchoring via π–cation, balanced by polar and alkyl contacts; minor clash with LYS156	**Strong**
HBMT-MA7	**–8.7**	ASP157, VAL136, GLY137, ARG60, PRO59, ALA302, GLY35, TRP38	H-bonding, π–cation, π–alkyl, van der Waals, positive–positive (repulsion)	Fills catalytic groove with strong hydrogen and π–cation interactions; minor repulsion from LYS156	**Strong**
Chloroquine*(Control)*	**–6.9**	VAL136, ASP342, TRP338, ALA424, ALA427, THR66, SER58	H-bonding, π–anion, π–π T-shaped, π–alkyl, van der Waals	Shallow binding with moderate π-stacking and anionic interactions; less polar anchoring than HBMT derivatives	**Moderate**
Quinine*(Control)*	**–8.4**	ASP342, VAL136, GLY137, ARG60, PRO59, ALA427, SER36	H-bonding, π–anion, π–alkyl, van der Waals, carbon H-bond, positive–positive (repulsion)	Deep binding via ASP342 with π–anion attraction; stable alkyl contacts; repulsion from ARG60 slightly impacts affinity	**Strong**

Table S4: Comparative Molecular Dynamics (500 ns) and MM/GBSA Analysis of HBMT Derivatives and Control Drugs with *P. falciparum* Malarial Protein (PDB ID: 5JWA)

Compound	Avg. RMSD (Å)	Avg. RMSF (Å)	Rg (Å)	Avg. H-Bonds	SASA (nm²)	MM/GBSA ΔGbind (kcal/mol)	Stability & Interaction Summary
HBMT3M4HB	2.10 ± 0.15	1.35 ± 0.08	20.1 ± 0.2	5–7	150.2 ± 2.3	–69.4	Highly stable conformation with dense H-bond network; consistent hydrophobic encapsulation of the aromatic core.
HBMT-MA3	2.25 ± 0.18	1.42 ± 0.09	20.3 ± 0.3	4–6	154.7 ± 2.0	–72.1	Slight backbone perturbation near LYS; most favorableΔGbind, reflecting enriched polar contacts and tight groove fitting.
HBMT-MA6	2.60 ± 0.20	1.56 ± 0.10	20.7 ± 0.2	3–5	159.6 ± 3.1	–61.8	Moderate RMSD increase localized around LYS156; π–cation stabilization persists throughout the simulation.
HBMT-MA7	2.48 ± 0.19	1.49 ± 0.11	20.5 ± 0.2	4–6	156.3 ± 2.8	–64.7	Strong π–cation and hydrogen bonding synergism; groove adaptation offsets transient electrostatic repulsion.
Chloroquine	3.10 ± 0.25	1.72 ± 0.12	21.3 ± 0.4	2–3	164.8 ± 3.4	–41.3	Highest conformational drift and SASA; reduced H-bonding suggests weak and less stable interaction profile.
Quinine	2.30 ± 0.17	1.45 ± 0.10	20.4 ± 0.2	3–4	158.0 ± 2.5	–58.9	Maintains consistent anchoring via

							ASP342; minor RMSD rise due to ARG60 fluctuations.

Table S5: In Silico Prediction of Membrane Permeability and Water Mapping Characteristics

Compound	logP_perm (cm/s)	ΔG_insert (kcal/mol)	Diffusion Coeff. ($\times 10^{-6}$ cm^2/s)	Desolvation Water Sites	Pocket Water Energy (ΔG_water, kcal/mol)	Membrane Permeability Potential
HBMT-MA3	–3.92	–4.1	1.02	4	–2.8, –2.3, –1.9, –1.7	Moderate
HBMT-MA6	–4.25	–4.5	0.88	5	–2.9, –2.6, –2.1, –1.8, –1.5	Moderate
HBMT-MA7	–3.75	–3.6	1.21	3	–2.5, –2.2, –1.7	Good
HBMT-3M4HB	–4.02	–4.2	0.96	4	–3.1, –2.7, –2.0, –1.9	Moderate
Chloroquine	–2.83	–2.4	1.56	2	–1.6, –1.5	High
Quinine	–3.11	–2.8	1.34	2	–1.9, –1.7	High

Table S6. Predicted ADME/T properties of HBMT Schiff base derivatives compared with chloroquine (reference).

Parameter	HBMT-3M4HB	HBMT-MA3	HBMT-MA6	HBMT-MA7	Chloroquine (Ref.)
Lipinski's Rule of 5	0 violations	0 violations	0 violations	0 violations	0 violations
Molecular Weight (g/mol)	447.5	430.5	415.5	429.5	319.9
LogP (Octanol/water)	2.7	2.5	2.9	3.1	3.3
Topological Polar Surface Area (TPSA, Å²)	104.3	96.8	92.5	98.7	48.6
Hydrogen Bond Donors/Acceptors	3/7	4/6	3/6	3/6	1/3
Rotatable Bonds	8	7	6	7	4
GI Absorption (SwissADME)	High	High	High	High	High
Oral Bioavailability (F%, predicted)	82	78	75	80	86
Caco-2 Permeability (10^{-6}	22.1	20.8	19.6	21.4	28.2

cm/s)					
P-glycoprotein Substrate	No	No	No	No	Yes
Plasma Protein Binding (%)	84	81	83	85	88
Blood–Brain Barrier Penetration	No	No	Borderline	No	Yes
CYP450 Inhibition	None	None	Weak CYP2C9	None	CYP2D6, CYP3A4
Predicted Clearance (CL, mL/min/kg)	14.2	13.8	15.6	14.7	12.1
Predicted Half-life (t½, h)	7.4	6.8	6.5	7.1	6.0
AMES Mutagenicity	Negative	Negative	Negative	Negative	Positive
Hepatotoxicity Risk	Low	Low	Moderate	Low	Moderate
Cardiotoxicity (hERG inhibition)	None predicted	None predicted	Weak	None predicted	Moderate
Skin Sensitization	Negative	Negative	Negative	Negative	Positive
Acute Oral Toxicity LD_{50} (rat, mg/kg)	1800	1750	1650	1720	950

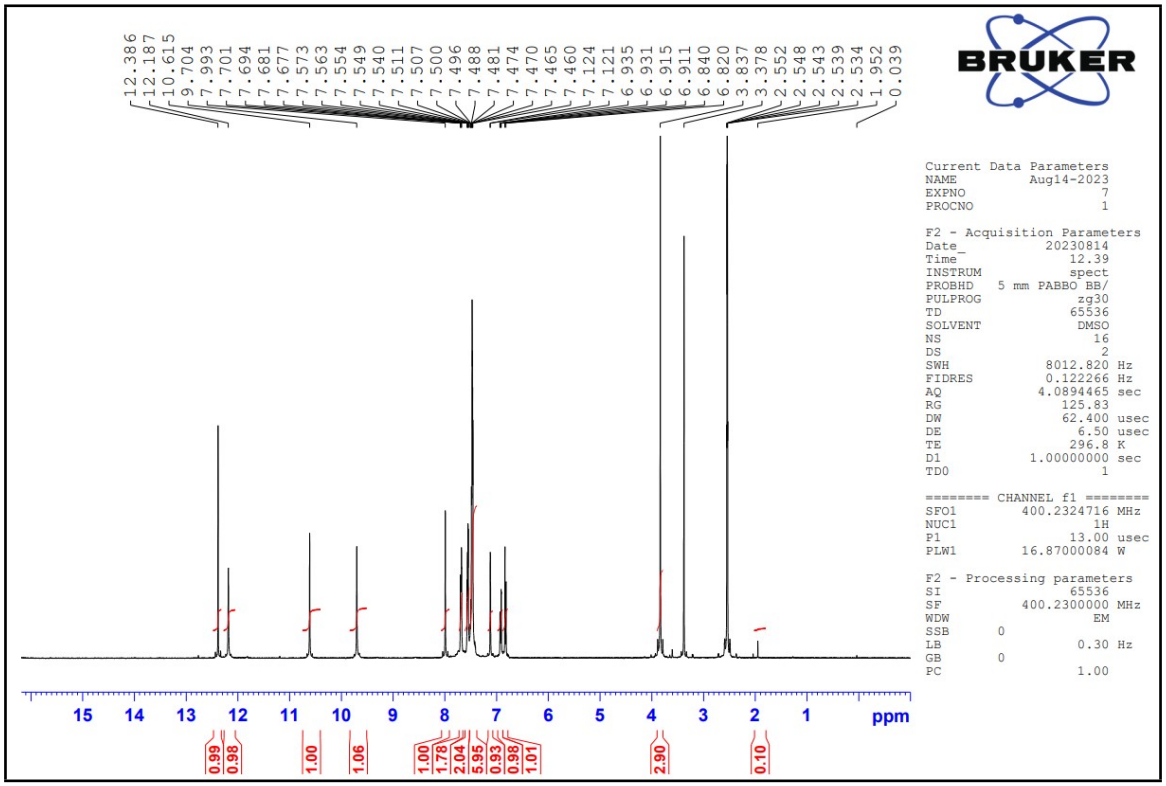

Fig.S1: ^{1}HNMR of HBMT-3M4HBin DMSO-d_6

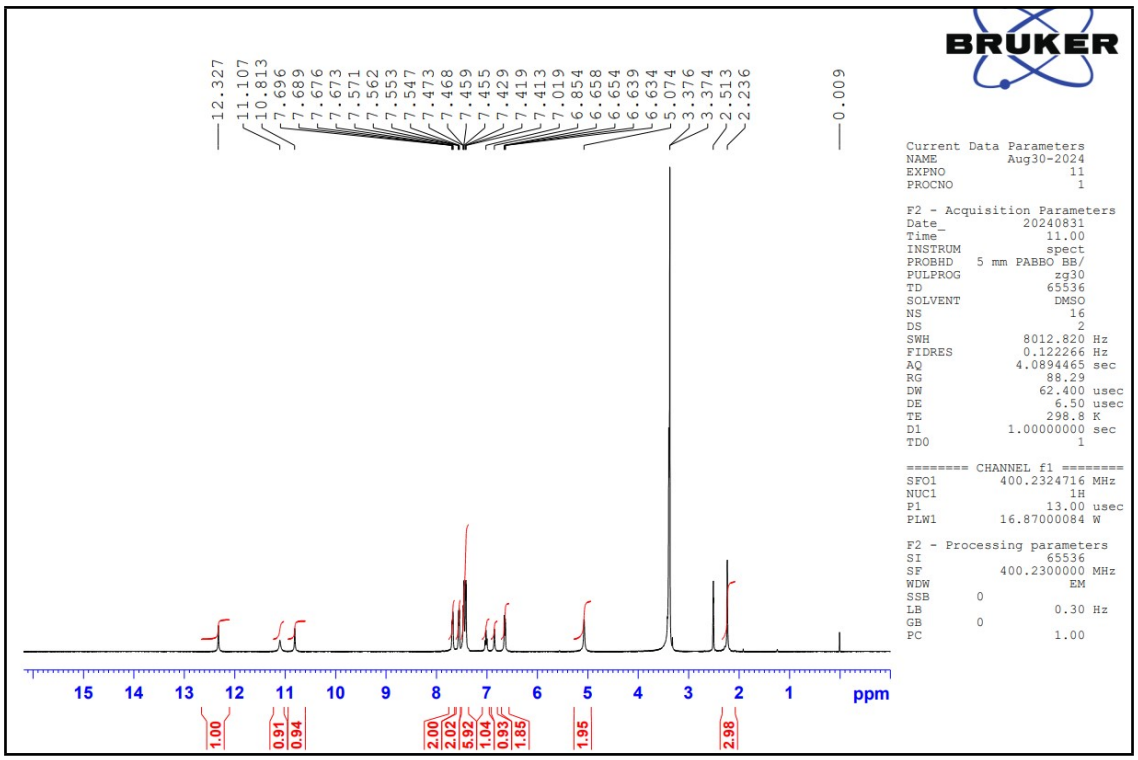

Fig. S2: ^{1}HNMR of HBMT-MA3in DMSO-d_6

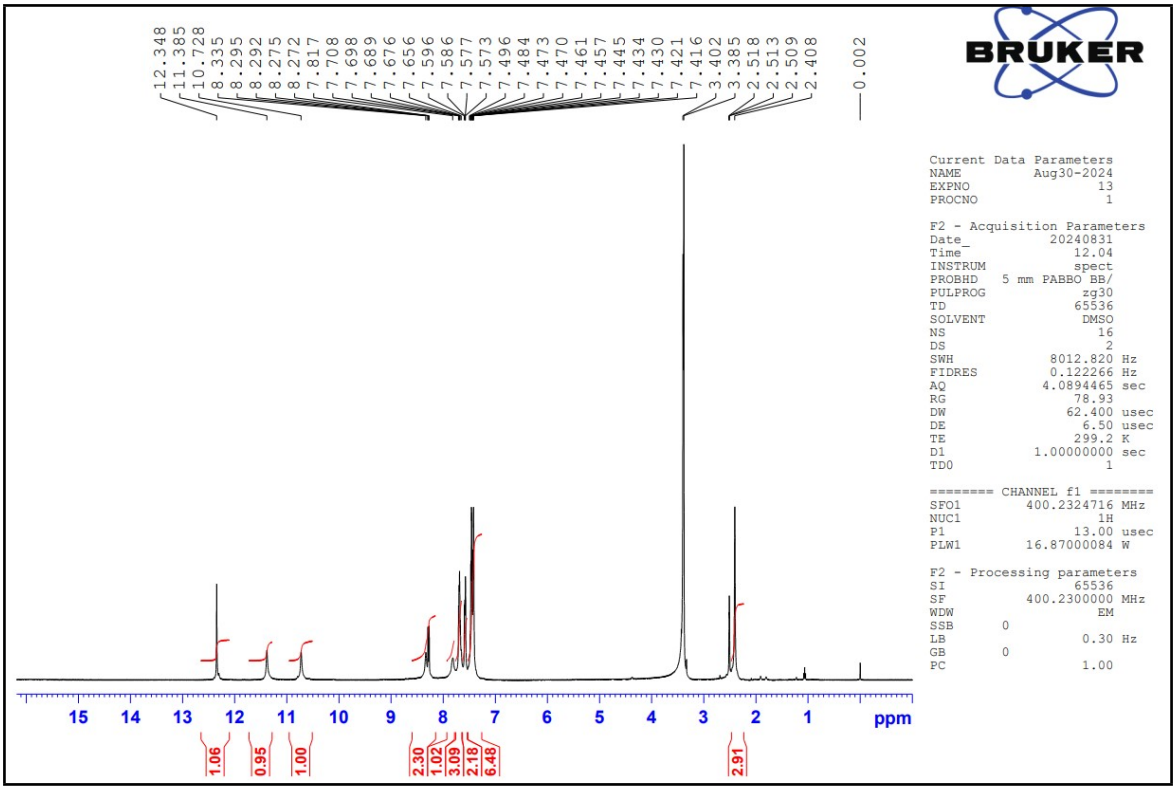

Fig. S3: ^{1}HNMR of HBMT-MA6in DMSO-d_6

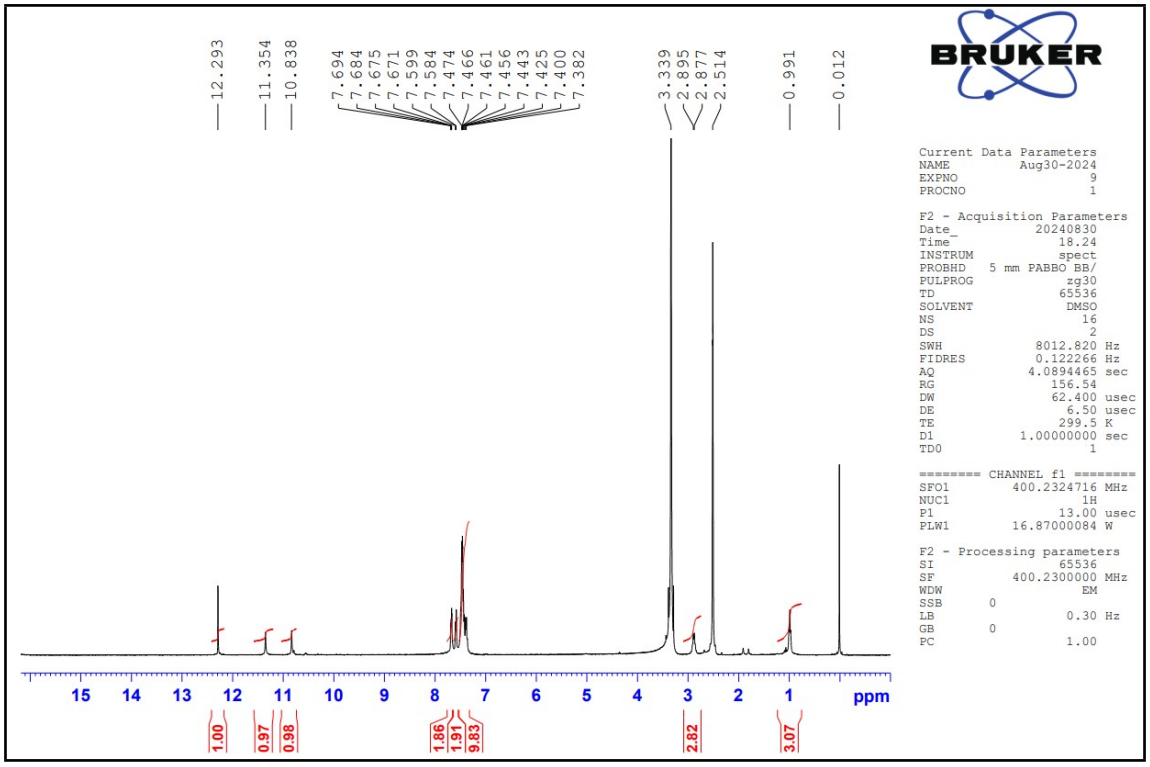

Fig. S4: ^{1}HNMR of HBMT-MA7in DMSO-d_6

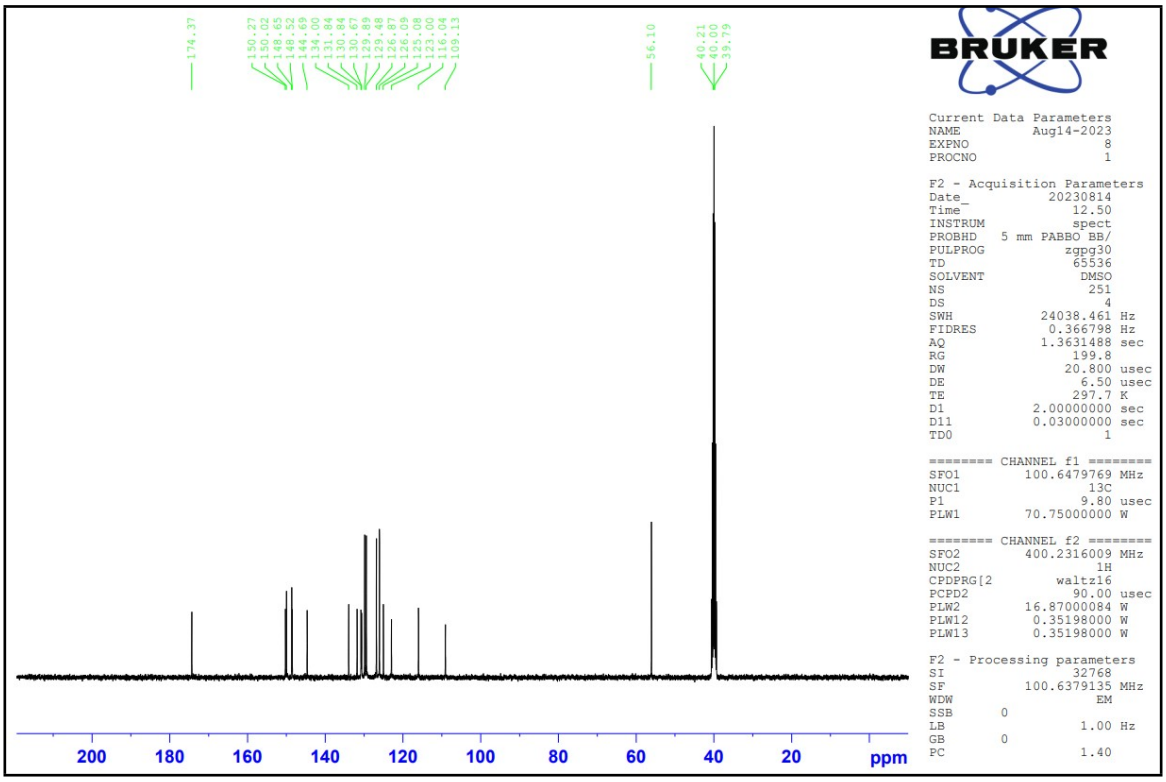

Fig. S5: ^{13}C NMR of HBMT-3M4HBin DMSO-d_6

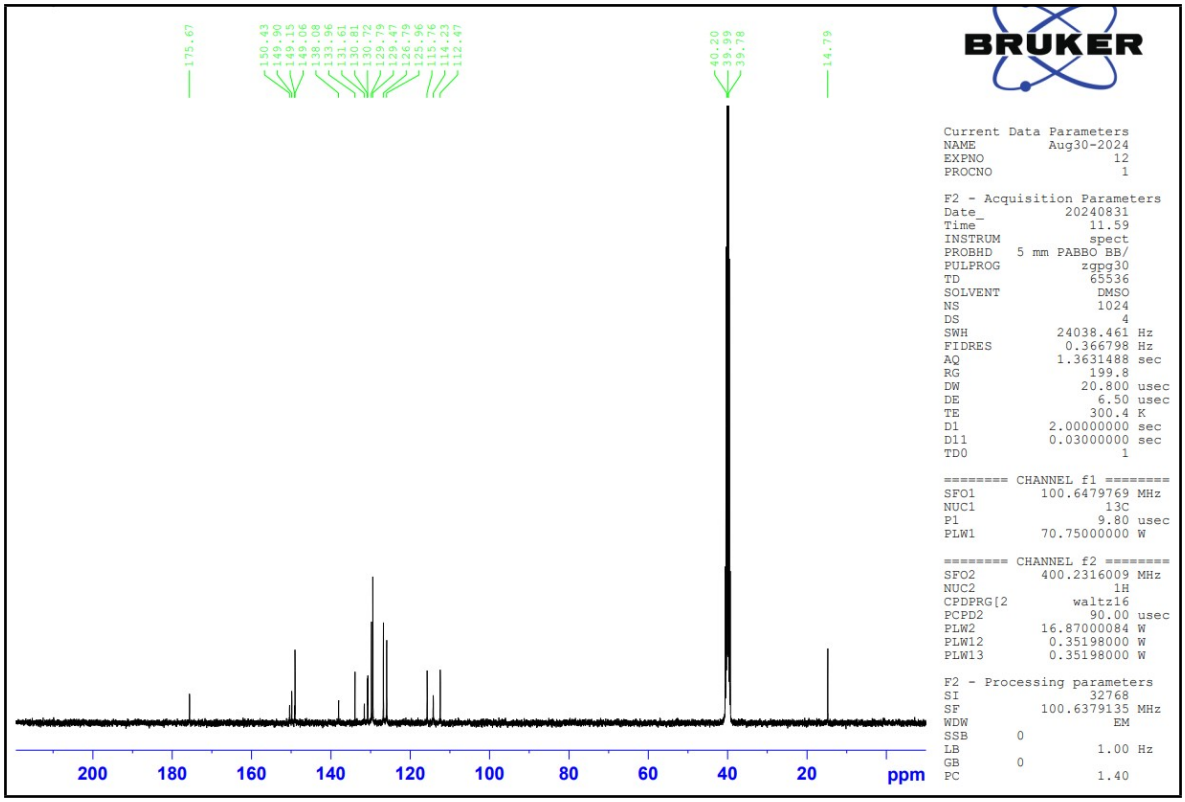

Fig. S6: ^{13}C NMR of HBMT-MA3in DMSO-d_6

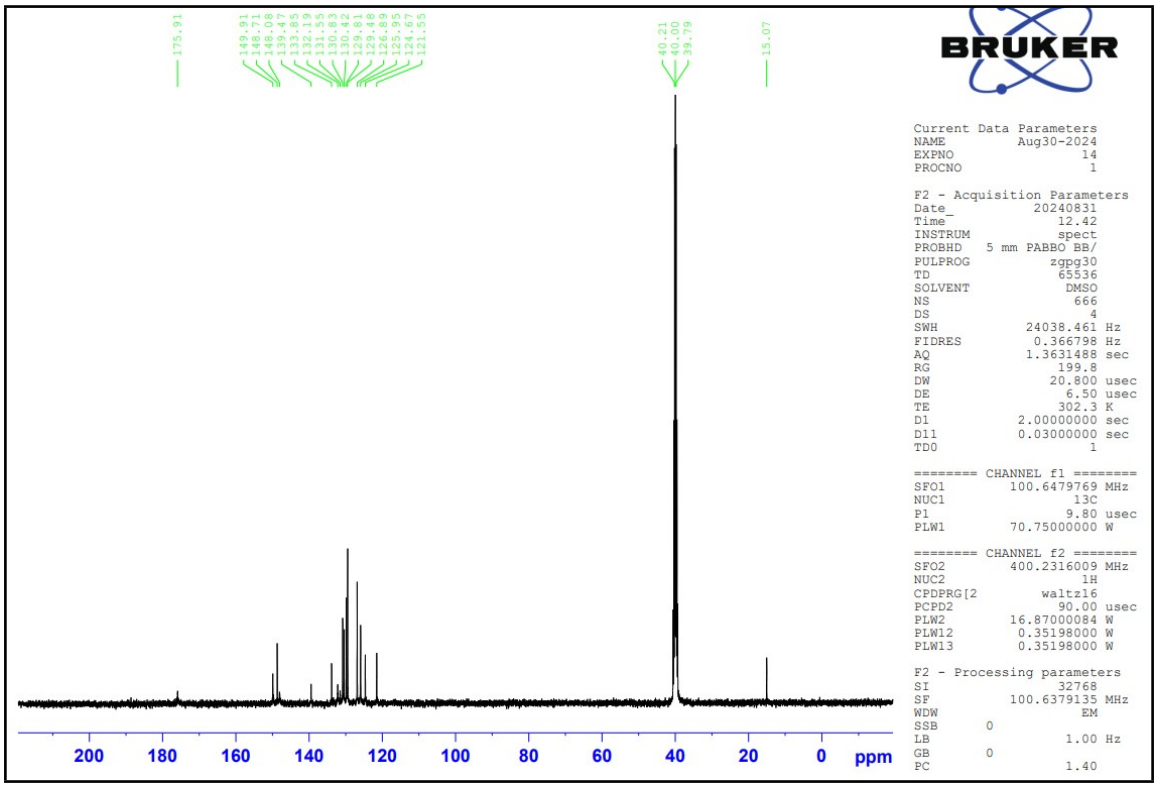

Fig. S7: ^{13}C NMR of HBMT-MA6in DMSO-d_6

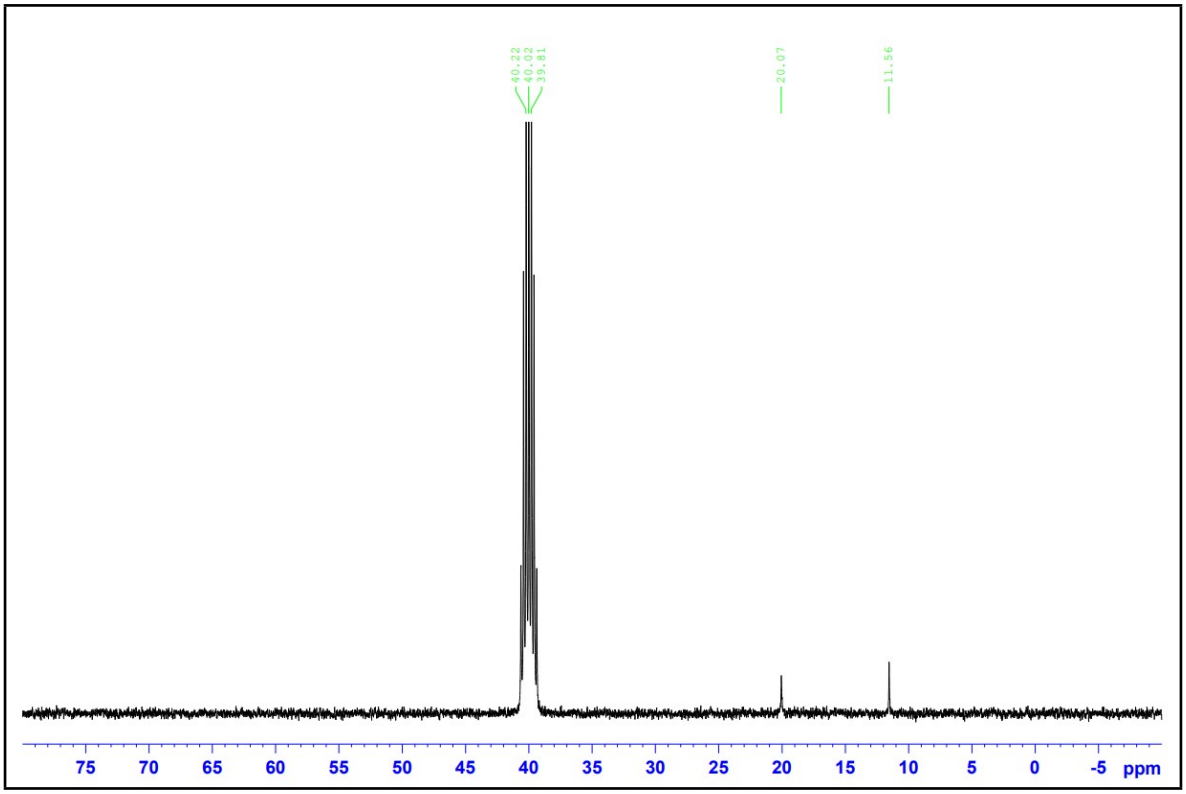

Fig. S8: ^{13}C NMR of HBMT-MA7 (1)in DMSO-d_6

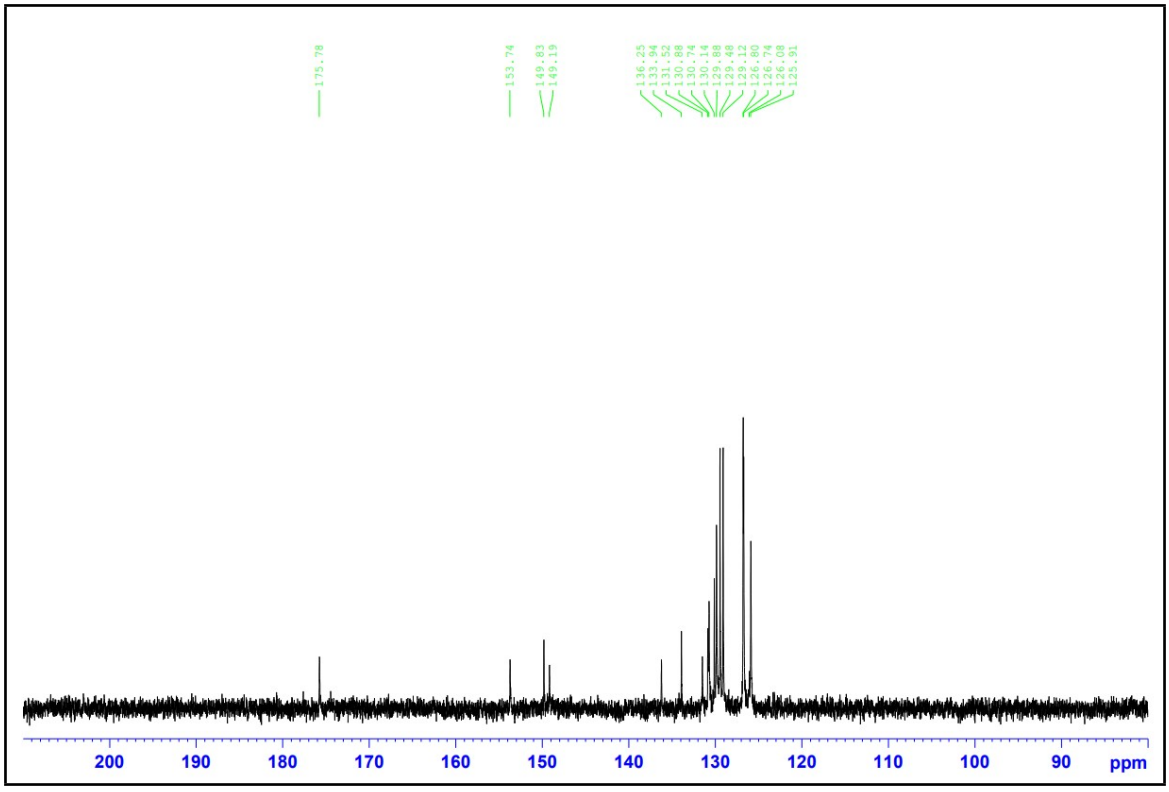

Fig. S9: ^{13}C NMR of HBMT-MA7 (2)in DMSO-d_6

Acquisition Parameter

Source Type	ESI	Ion Polarity	Positive	Set Nebulizer	1.2 Bar
Focus	Active	Set Capillary	4500 V	Set Dry Heater	200 °C
Scan Begin	20 m/z	Set End Plate Offset	-500 V	Set Dry Gas	7.0 l/min
Scan End	1200 m/z	Set Charging Voltage	2000 V	Set Divert Valve	Source
		Set Corona	0 nA	Set APCI Heater	0 °C

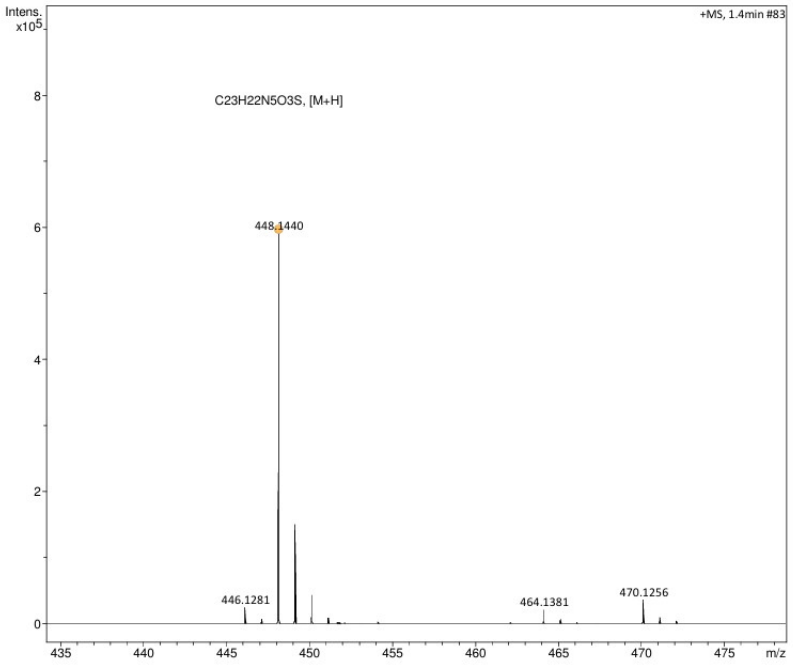

Fig. S10: Mass spectrum of HBMT-3M4HB

Acquisition Parameter

Source Type	ESI	Ion Polarity	Positive	Set Nebulizer	0.9 Bar
Focus	Active	Set Capillary	4500 V	Set Dry Heater	200 °C
Scan Begin	20 m/z	Set End Plate Offset	-500 V	Set Dry Gas	7.0 l/min
Scan End	1200 m/z	Set Charging Voltage	2000 V	Set Divert Valve	Source
		Set Corona	0 nA	Set APCI Heater	0 °C

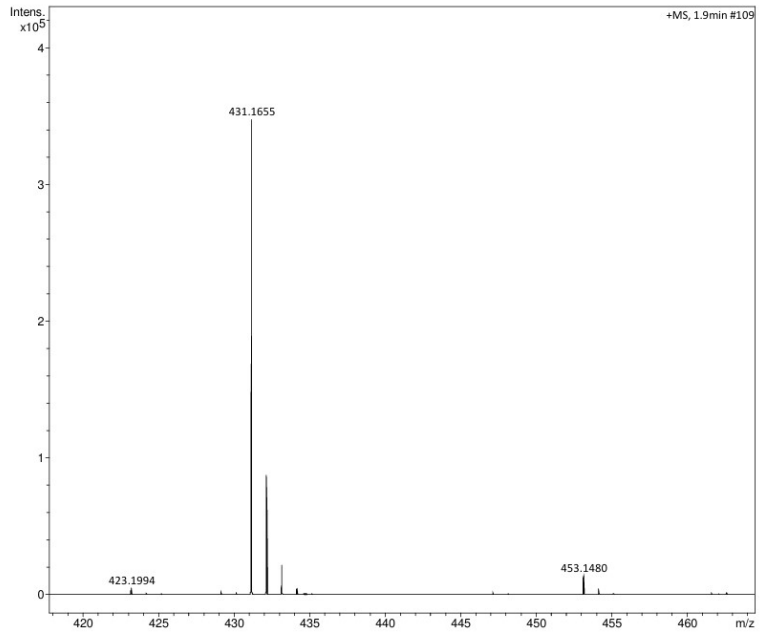

Fig. S11: Mass spectrum of HBMT-MA3

Acquisition Parameter

Source Type	ESI	Ion Polarity	Positive	Set Nebulizer	1.2 Bar
Focus	Active	Set Capillary	4500 V	Set Dry Heater	200 °C
Scan Begin	20 m/z	Set End Plate Offset	-500 V	Set Dry Gas	7.0 l/min
Scan End	1200 m/z	Set Charging Voltage	2000 V	Set Divert Valve	Source
		Set Corona	0 nA	Set APCI Heater	0 °C

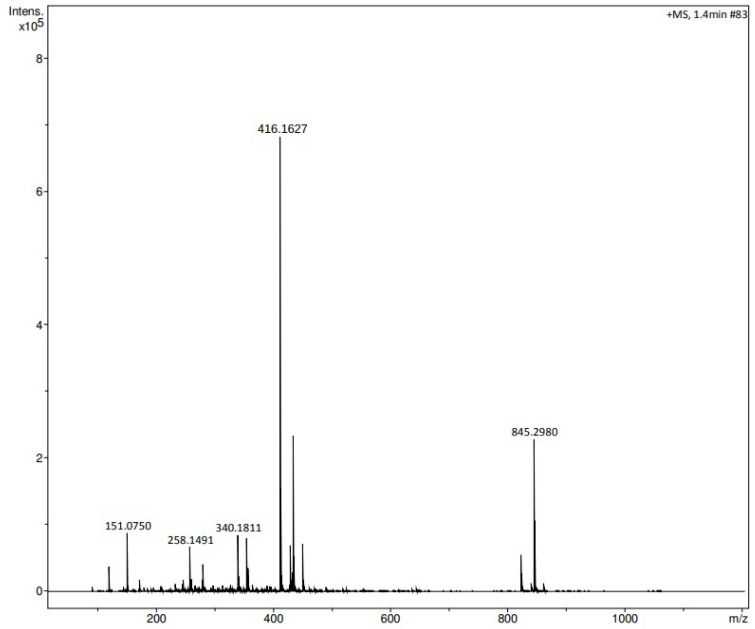

Fig. S12: Mass spectrum of HBMT-MA6

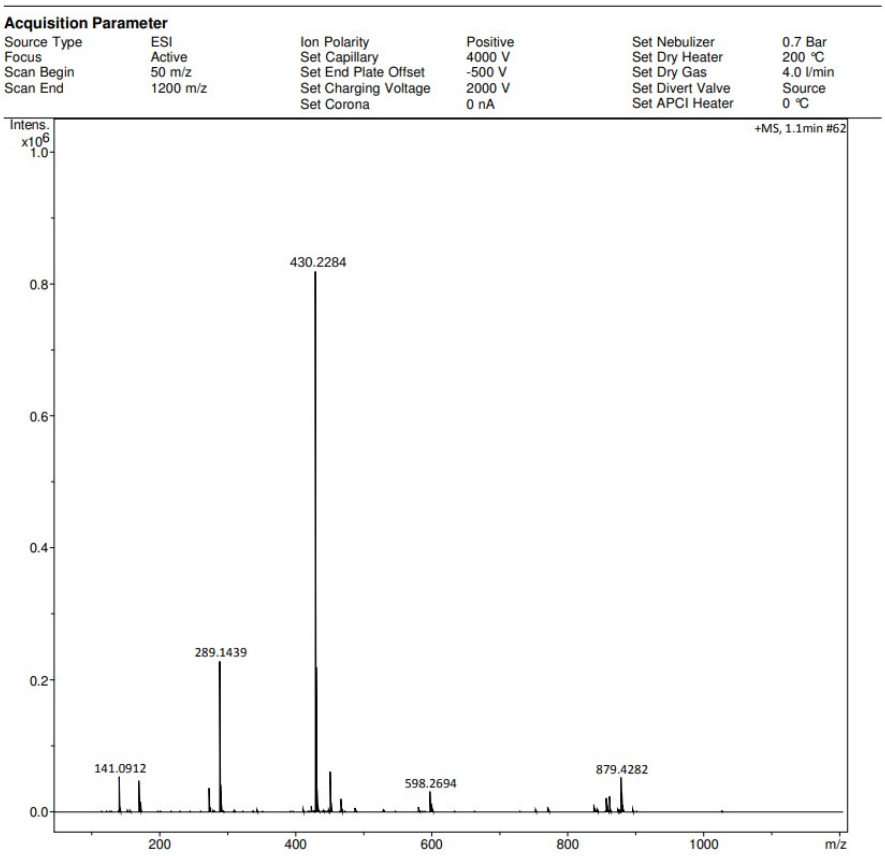

Fig. S13: Mass spectrum of HBMT-MA7

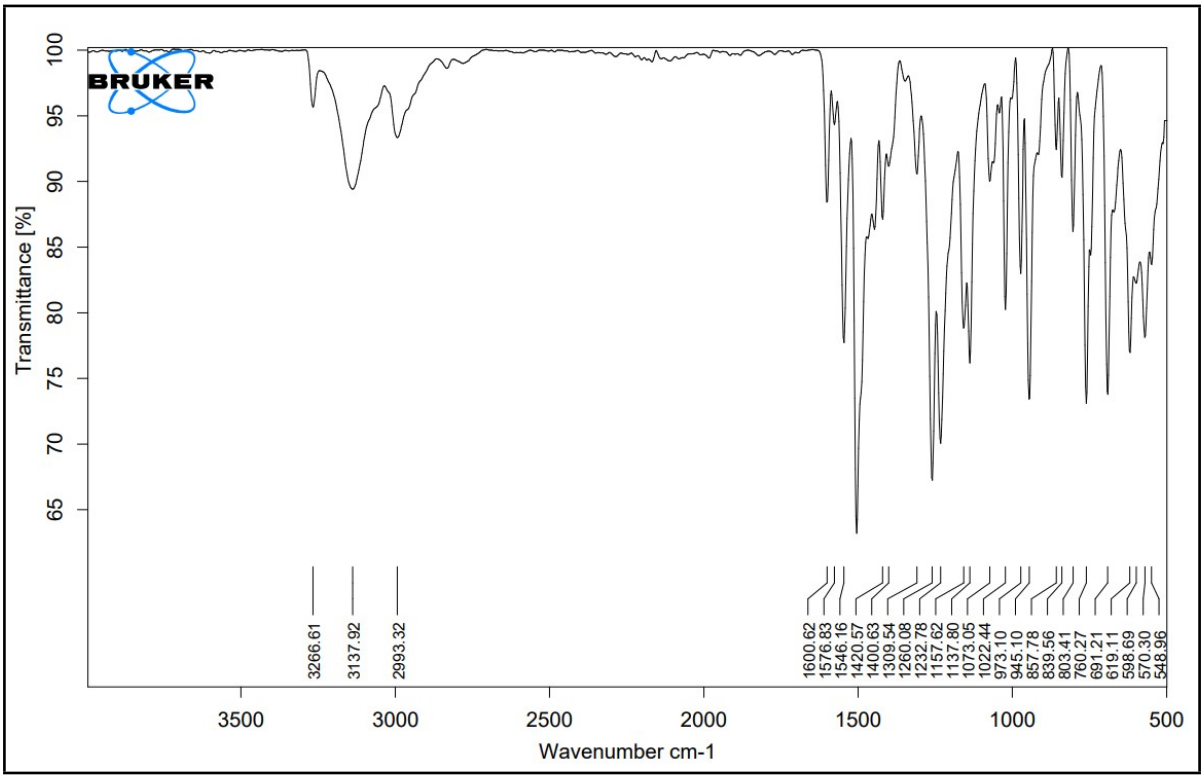

Fig. S14: IR spectra of HBMT-3M4HB

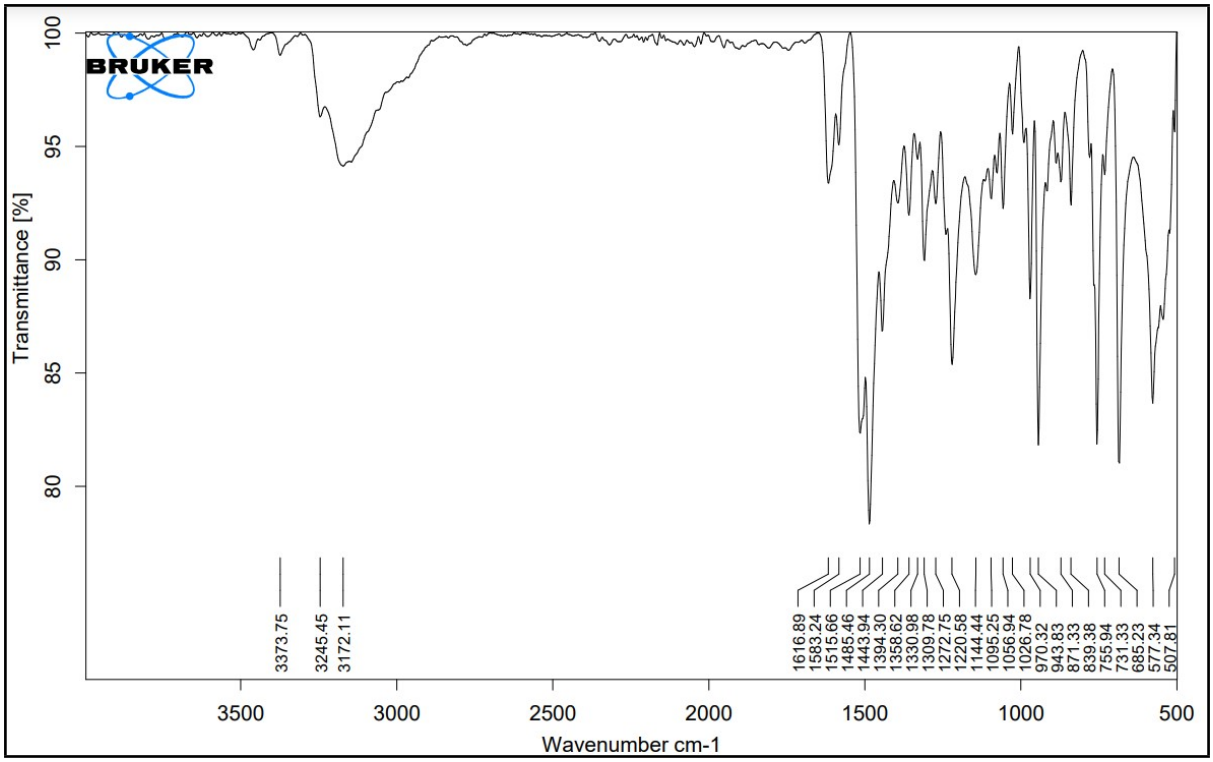

Fig.S15: IR spectra of HBMT-MA3

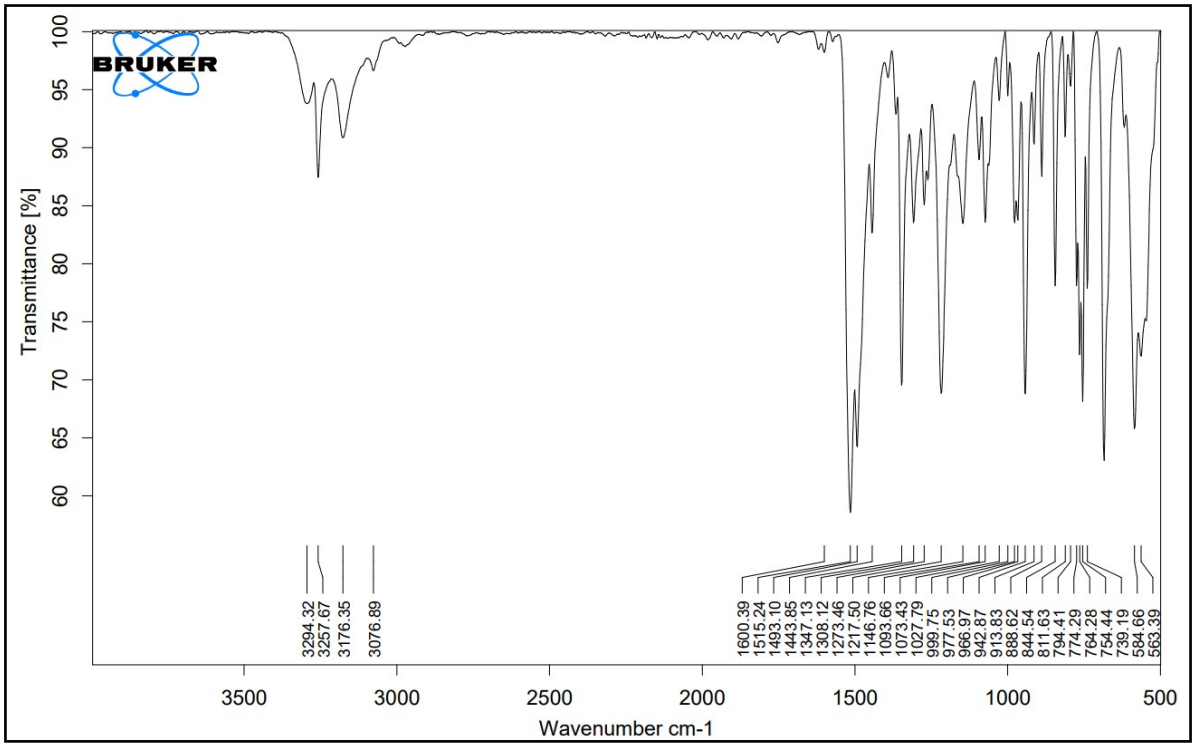

Fig.S16: IR spectra of HBMT-MA6

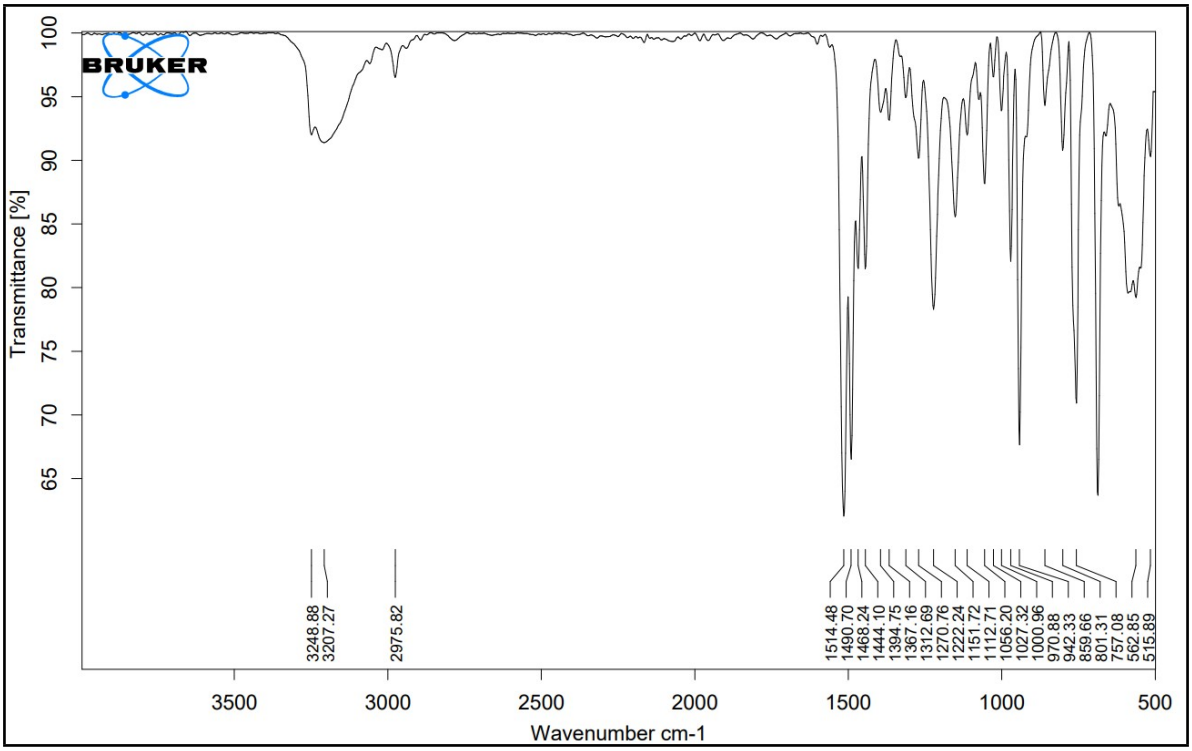

Fig.S17: IR spectra of HBMT-MA7

*Document: 17 06 2025 (*VarioMICRO CHNS analyzer*) from 17/06/2025 10:23:57 AM*

VarioMICRO CHNS analyzer

Compound Name: SL5

Statistic report

Name	C [%]	H [%]	N [%]	S [%]
Run-1	61.693	4.722	15.630	7.153
Run-2	61.690	4.721	15.628	7.152
Mean Value	61.692	4.722	15.629	7.153
Deviation, abs.	0.002	0.001	0.001	0.001
% RSD	0.34%	1.50%	0.90%	0.99%

Fig. S18: CHNS data of HBMT-3M4HB

*Document: 12 03 2025 (*VarioMICRO CHNS analyzer*) from 12/03/2025 10:46:21 AM*

VarioMICRO CHNS analyzer

Compound Name: MA3

Statistic report

Name	C [%]	H [%]	N [%]	S [%]
Run-1	64.166	5.148	19.513	7.449
Run-2	64.163	5.149	19.511	7.448
Mean Value	64.165	5.149	19.512	7.449
Deviation, abs.	0.002	0.001	0.001	0.001
% RSD	0.33%	1.37%	0.72%	0.95%

Fig. S19: CHNS data of HBMT-MA3

*Document: 12 03 2025 (*VarioMICRO CHNS analyzer*) from 12/03/2025 11:07:11 AM*

VarioMICRO CHNS analyzer

Compound Name: MA6

Statistic report

Name	C [%]	H [%]	N [%]	S [%]
Run-1	66.465	5.088	16.849	7.718
Run-2	66.466	5.089	16.850	7.717
Mean Value	66.466	5.089	16.850	7.718
Deviation, abs.	0.001	0.001	0.001	0.001
% RSD	0.11%	1.39%	0.42%	0.92%

Fig. S20: CHNS data of HBMT-MA6

*Document: 12 03 2025 (*VarioMICRO CHNS analyzer*) from 12/03/2025 11:46:05 AM*

VarioMICRO CHNS analyzer

Compound Name: MA7

Statistic report

Name	C [%]	H [%]	N [%]	S [%]
Run-1	67.093	5.396	16.284	7.455
Run-2	67.095	5.397	16.283	7.456
Mean Value	67.094	5.397	16.284	7.456
Deviation, abs.	0.001	0.001	0.001	0.001
% RSD	0.21%	1.31%	0.43%	0.95%

Fig. S21: CHNS data of HBMT-MA7

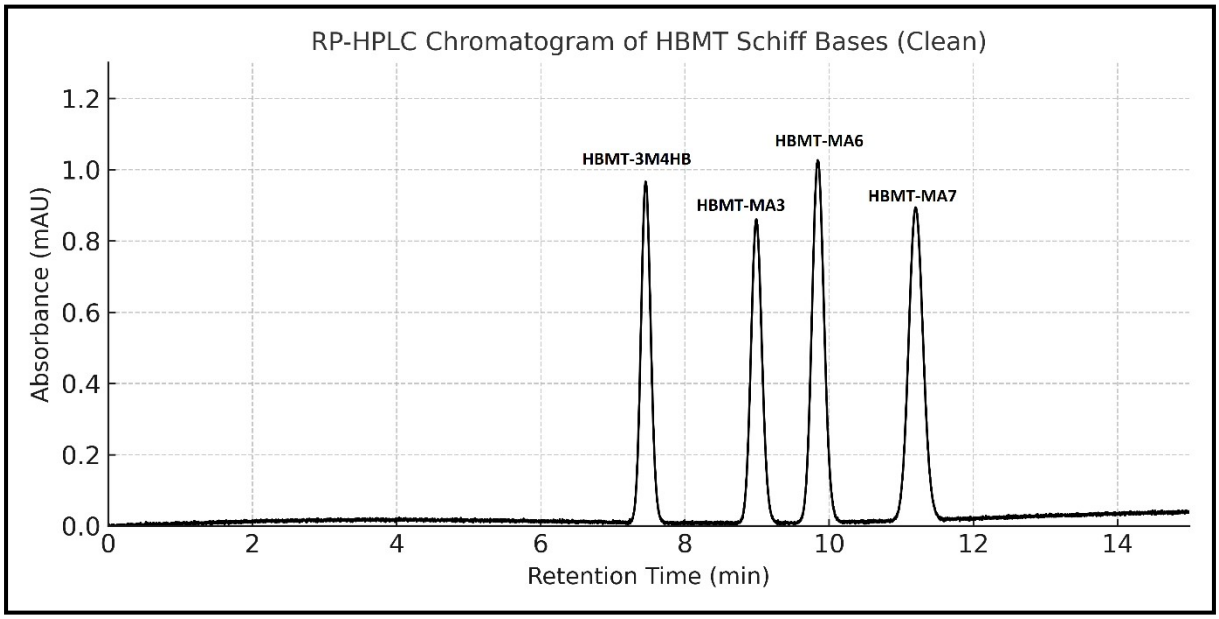

Fig. S22: Representative RP-HPLC chromatogram (UV 290 nm) of HBMT Schiff bases showing baseline-resolved peaks at 7.42, 8.95, 9.80, and 11.15 min. All analytes exhibited chromatographic purity above 98.8%.